Structures 70 (2024) 107761

Contents lists available at ScienceDirect

Structures

journal homepage: www.elsevier.com/locate/structures

Dynamic system identification by the frequency response matrix

M. Cacho-Pérez[1]

ITAP. University of Valladolid, Paseo del Cauce 59, 47011, Valladolid, Spain

ARTICLE INFO

Keywords:
Dynamic system identification
Residues and poles form
Frequency response function (FRFs) rational approximation
Frequency domain analysis
Real and imaginary FRFs parts fitting
Analytic complex functions residues

ABSTRACT

This work estimates the residues and poles of the dynamic system to express the terms of the frequency response matrix as the sum of simple fractions (each vibration mode contributes two terms). The starting point is the acceleration response at various points of the structure, it is integrated twice and an analysis is performed in the frequency domain. The measured vibration frequencies, damping factors, and residues are estimated by least squares fitting of the measured or experimental frequency response functions (FRFs). The damping of the structure or system can be proportional or general. The dynamic system is identified by relating the residues of the functions of the frequency response matrix (complex functions) with the residues measured from the outputs of the system excited by forces/inputs of impulse, sinusoidal, frequency sweep or other type.

1. Introduction

The behavior of dynamic systems can be described by the equations of motion obtained systematically from Lagrange's equations [1]. However, its representation as a Transfer Function Matrix (TFM) or State Space Model (SSM) is much more interesting from the point of view of control theory, which can be achieved by knowing the zeros, poles and gains or residues and poles of the dynamic system. To achieve this objective, identify the dynamic system, on the one hand there are techniques that aim to update an initial computational or numerical model to adapt it to the experimental results; and on the other hand those techniques that are based on estimating a new model representation without the need to previously build a computational model. In the context of a multi-input, multi-output (MIMO) system, the Transfer Function Matrix represents the relationship between the inputs and outputs of the system [2–4]. The State Space Model is a mathematical framework used to describe and analyze dynamic systems. It provides a set of first-order differential (or difference) equations that represent the system's evolution over time, capturing both its dynamics and its internal state [5–7].

The first group of methods, called Finite Element Model Updating (FEMU) is a technique used to refine and improve the accuracy of a finite element model by comparing its predictions with experimental data. This process involves adjusting the parameters of the model to minimize the discrepancy between simulated results and real-world observations and provide good results after a long iterative updating process. These techniques begin creating an initial finite element model based on theoretical knowledge and design specifications with a certain number of structural elements that have some provisional properties. Then compare the experimental data with the results predicted by the finite element model and identify discrepancies or differences. After updating, validate the refined model by comparing its predictions with additional experimental data or by performing new tests and if the updated model still does not sufficiently match experimental data, iterate the updating process by refining the model further and re-evaluating. This numerical model requires the adjustment of so many parameters and there is so much uncertainty regarding the physical properties that it is not practical [8–11].

On the other hand, in the 1990s, Yang and Yeh [12] worked with complex data from FRFs for proportional damping using the properties of the Hankel matrix and the singular value decomposition technique. Chen et al. [13] identified the general damping matrix and then the mass and stiffness matrix. Their methodology was based on a least squares minimization approach for the error between the experimental and estimated frequency response functions of the structure. Angelis et al. [14] proposed a methodology based on an estimated representation of the state space of a proportionally damped system. And they discuss the minimum number of sensors and actuators needed to obtain a unique solution to the problem. These techniques are called Modal Parameter Extraction methods and directly estimate the dynamic model from experimental data without the need to perform complex or highly detailed iterative computational model updating processes [15–20]. Modal parameters extraction involves determining the dynamic characteristics of a system, such as natural frequencies, mode shapes, and damping ratios. These parameters are crucial for understanding the vibrational behavior of structures and systems, and they are often used in structural analysis, design optimization, and health monitoring.

E-mail address: mariano.cacho@uva.es.
[1] Ph.D. Industrial Engineering.

https://doi.org/10.1016/j.istruc.2024.107761
Received 18 July 2024; Received in revised form 17 September 2024; Accepted 4 November 2024
Available online 15 November 2024

A promising research direction is the development of a reverse identification method that integrates real-time response measurements and the physical laws governing structural systems to deduce time-domain evolution and frequency-domain statistical characteristics. Traditional model-driven methods involved several steps, including model updating, optimal sensor placement [21] and external load inversion [22]. On the other hand, emerging data-driven methods aim to create deep learning ensemble models to approximate mathematical expressions between system inputs and outputs [23]. Given the limitations of the inverse modal transformation in model-driven methods Liu et al. develops a hybrid model-data-driven framework based on physics-informed neural network and improved Kalman filter algorithm [24].

In recent years, structural vibration control has rapidly developed into a new advanced seismic design method. Structural vibration control is to arrange seismic isolation and energy dissipation devices on the building structures to reduce or suppress the structural dynamic response. Dong et al. aims to develop a high-performance acrylate viscoelastic damper, which is suitable for the low-frequency vibration control of building structures. The analysis results show that the proposed model can describe the influence of ambient temperature, excitation frequency and displacement amplitude [25].

The objective of this work is first to identify the dynamic system in the form of a Transfer Function Matrix (TFM). This magnitude is a fundamental in control systems and structural dynamics that describes the relationship between input and output variables of a system in the frequency domain. It provides a comprehensive way to analyze and understand the system's dynamic behavior. And secondly, being able to predict the dynamic behavior of the system for any other set of input signals (all types of dynamic simulations), which also allows knowing the dynamic system to apply vibration control techniques in slender structures. The methodology applies to both the case of proportional viscous damping and the case of non proportional or general damping.

The main contributions and novelties of this paper are summarized as follows:

1. Using advanced numerical techniques (Least-Squares Rational Function estimation (LSRF) and FRFs Least-Squares Fitting methods), the poles and residues of the mechanical system are obtained in the frequency range of interest from the forces and accelerations in the sensors.
2. Residues ($\boldsymbol{r}_{iq}^{(k)}$) are calculated as differences between observed and estimated values (see Methodology, Fig. 1).
3. The major contribution of this work is the calculation of the residues of the estimated FRFs (${}_k\hat{\boldsymbol{A}}_{ij}$) as complex analytical functions that define the dynamic system (see Methodology, Fig. 1).

In order to validate the methodology of this work, the mass, damping and stiffness matrices are given as data, the system is excited with a force in a certain position and the corresponding synthetic records of accelerations in the positions of the sensors are obtained. It is integrated numerically to obtain displacements, the synthetic FRFs are calculated, the poles of the system are estimated and then both the real and the imaginary part of the measured FRFs are adjusted to a nonlinear rational form model based on the poles of the system, to obtain the measured residues.

This article has been organized as follows: after this brief introduction, the methodology used is summarized and synthetic data is generated for a given case for which the methodology is applied. Finally, the main conclusions and contributions of the work are listed.

2. Methodology

This section summarizes the methodology for performing a frequency domain fitting of the dynamic behavior of the mechanical system (n degrees of freedom and truncated to m modes). Fig. 1 shows a flowchart that helps understand the methodology of this section. The objective is to obtain the transfer functions to identify the dynamic system by follow the next steps:

1. The starting point is the acceleration records of a dynamic system (for example, a structure) at certain points caused by a force (an impact, for example) at one of the points where it is being measured (driving point).
2. A sampling rate f_s is established and sensors records saved every T_s seconds (it is known that $T_s = 1/f_s$).
3. Integrate the accelerations to obtain the displacements in those same locations (Matlab™→ *convertVibration*()) [26,27].
   The magnitudes are defined in the complex domain, the variable $s \in \mathbb{C}$ and $h_{ij}(s)$ are complex analytical functions.
4. Apply the Fast Fourier Transform (FFT) to the input (at node q) and the outputs (at node i) to calculate the Frequency Response Functions (measured FRFs) $h_{iq}(i\omega)$.
5. System poles $s = p_k$ are estimated, for this the Least-Squares Rational Function estimation method (LSRF) is used (Matlab™→ *modalfit*()) [27–29].
6. A nonlinear least squares for the measured FRFs is carried out. Using an expanded matrix, both its real part and the complex part are adjusted and the residues are estimated.
   It is important to point out that the estimated complex values the measured residues $\boldsymbol{r}_{iq}^{(k)}$ and do not coincide with the values of the residues ${}_k\hat{\boldsymbol{A}}_{ij}$ of the complex functions $h_{ij}(s)$ that define the dynamic system.
7. From the measured residues, the complex residues of the transfer functions that relate response at i with input at node q are calculated:
$$\hat{\boldsymbol{R}}_{iq}^{(k)} = \boldsymbol{r}_{iq}^{(k)} \cdot T_s = \frac{\boldsymbol{r}_{iq}^{(k)}}{f_s} \tag{1}$$
8. All terms of the matrix $\hat{\boldsymbol{H}}(s)$ can be calculated from a single row $\hat{h}_{qi}(s)$ or a single column $\hat{h}_{iq}(s)$, due to the reciprocity property [15,16,30], from all residues tensors:
$${}_k\hat{\boldsymbol{A}}_{ij} = \frac{\hat{\boldsymbol{R}}_{iq}^{(k)} \cdot \left(\hat{\boldsymbol{R}}_{iq}^{(k)}\right)^T}{\hat{R}_{qq}^{(k)}} \tag{2}$$
   where $\hat{\boldsymbol{R}}_{qq}^{(k)}$ is the residue for mode k corresponding to the driving point (output at q for input at q too) and $()^T$ denotes the operation of transposing a vector or a matrix (a vector in this specific case). Logically, it must be fulfilled:
$${}_k\hat{\boldsymbol{A}}_{iq} = \hat{\boldsymbol{R}}_{iq}^{(k)} \tag{3}$$
   These mathematical operations make it easy to calculate the residues of the Transfer Function Matrix:
$$\hat{\boldsymbol{H}}(s) = \hat{h}_{ij}(s) = \sum_{k=1}^{m} \frac{{}_k\hat{\boldsymbol{A}}_{ij}}{s - p_k} + \frac{{}_k\hat{\boldsymbol{A}}_{ij}^*}{s - p_k^*} \tag{4}$$
   where the symbol $()^*$ represents the complex conjugate number.

The methodology presented allows the identification of the dynamic system in the s-domain through a Transfer Function Matrix, which makes it possible to convert it to State Space Model and perform dynamic simulations/predictions and vibration control of the structures.

3. Results and discussion

In this section, the methodology of this work will be applied to a dynamic system with three degrees of freedom, for which data on the mass, damping and stiffness matrices are provided. Two cases of damping will be considered, proportional and general (or non-proportional damping).

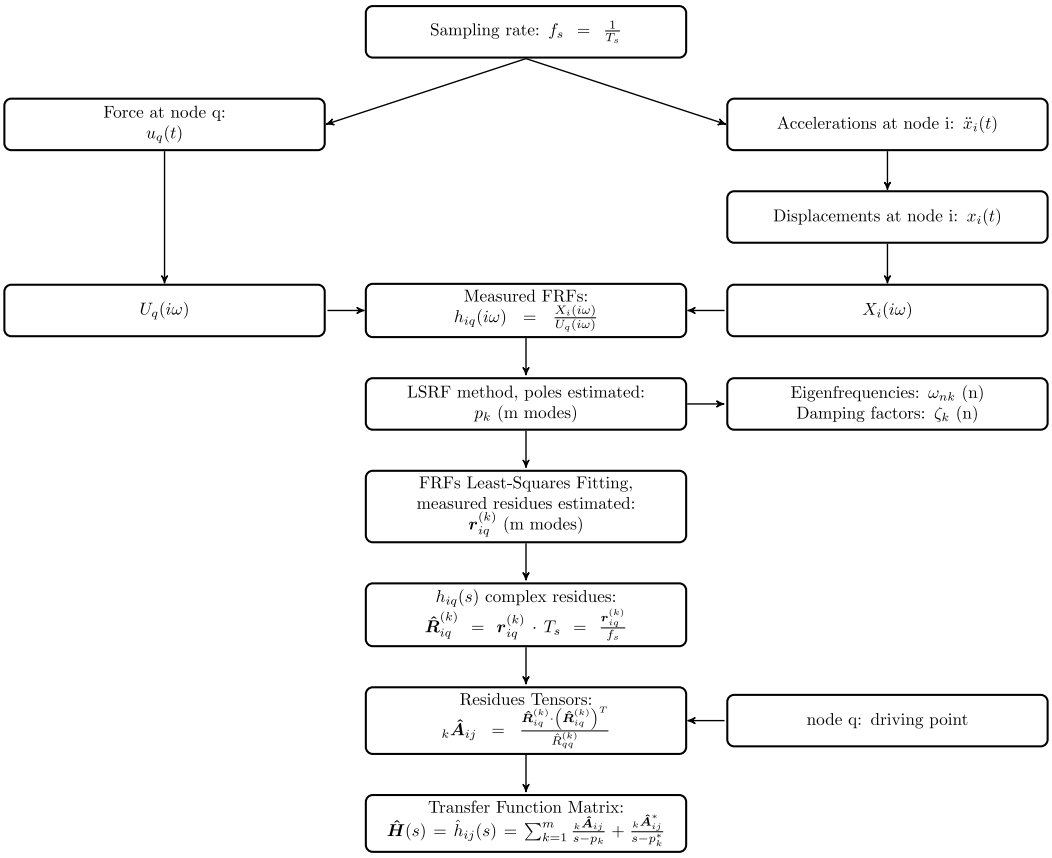

Fig. 1. Numerical dynamic system identification.

3.1. Problem data

The data of the cases that will be analyzed below are:

$$\boldsymbol{M} = \begin{bmatrix} 2.0 & 0.0 & 0.0 \\ 0.0 & 1.5 & 0.0 \\ 0.0 & 0.0 & 1.0 \end{bmatrix}; \quad \boldsymbol{K} = \begin{bmatrix} 800.0 & -320.0 & 0.0 \\ -320.0 & 450.0 & -200.0 \\ 0.0 & -200.0 & 200.0 \end{bmatrix};$$
$$\boldsymbol{C}_p = 0.01 \cdot \boldsymbol{K} = \begin{bmatrix} 8.0 & -3.2 & 0.0 \\ -3.2 & 4.5 & -2.0 \\ 0.0 & -2.0 & 2.0 \end{bmatrix}; \quad \boldsymbol{C}_g = \begin{bmatrix} 2.0 & -2.0 & 3.0 \\ -2.0 & 5.0 & -4.0 \\ 3.0 & -4.0 & 5.0 \end{bmatrix} \tag{5}$$

where $\boldsymbol{M}, \boldsymbol{K}$ are the mass and stiffness matrices, $\boldsymbol{C}_p$ is the damping matrix for the case of proportional damping and $\boldsymbol{C}_g$ is the damping matrix for the case of non-proportional or general type damping.

Regarding the excitation, an impact (impulse type) is used at the initial instant applied to node 1: $u_q(t) = F_0 \cdot \delta(t)$ with $F_0 = 1.0\,\text{N}$ and $\delta(t)$ is the Dirac delta function. Sampling rate $f s = 2000\,\text{Hz}$; sampling time $T_s = 0.0005\,\text{s}$; and final time $t_f = 120\,s$.

3.2. Proportional damping case

In this section the system will be identified from the records of displacements in the degrees of freedom of the dynamic system due to an impact at the first degree of freedom (11 is the driving point). Fig. 2 shows the synthetic displacements records that correspond to the case of proportional damping, impulse input at node 1 and sampling rate f_s.

The analysis in the frequency domain is carried out and the poles of the system are calculated (being n the number of degrees of freedom and m the number of modes, in this case $n = m = 3$). The LSRF method (see flowchart 1) is applied:

$$\begin{aligned} p_1 &= -0.1968 + 6.27i \\ p_2 &= -1.447 + 16.95i \\ p_3 &= -2.856 + 23.73i \end{aligned} \tag{6}$$

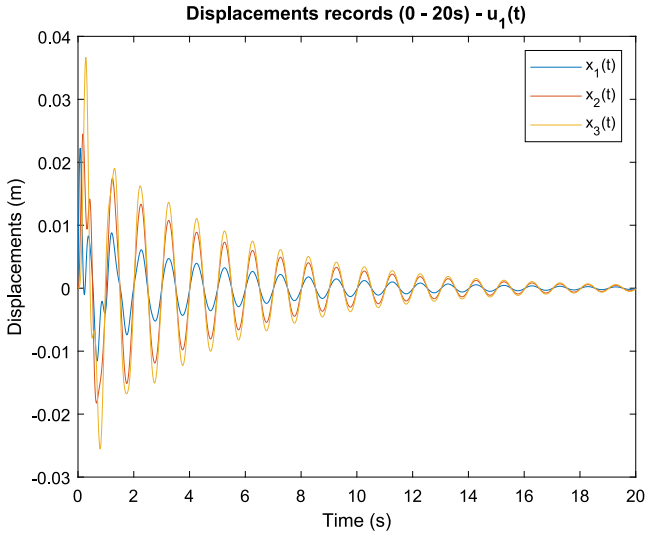

Fig. 2. Displacements records, impulse force at 1. (For interpretation of the references to color in this figure legend, the reader is referred to the web version of this article.)

note that for simplicity only three poles have been indicated (those with the positive imaginary part), the other three poles are the corresponding complex conjugate numbers of those indicated above. The symbol i denotes the imaginary unit $i = \sqrt{-1}$.

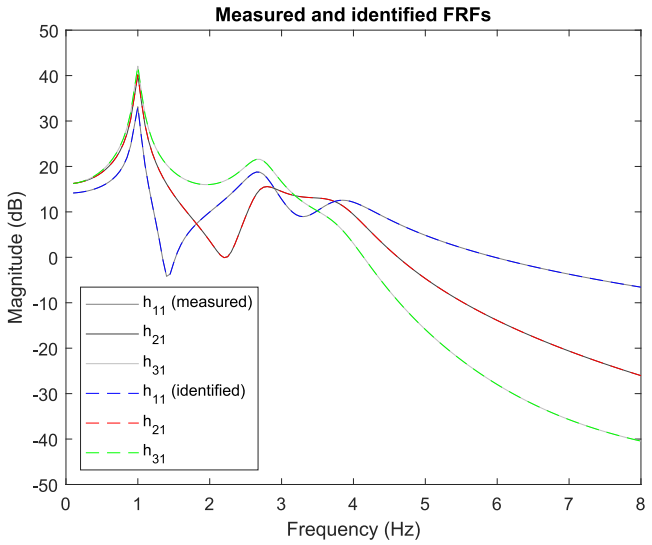

Fig. 3. Measured and identified FRFs (proportional damping). (For interpretation of the references to color in this figure legend, the reader is referred to the web version of this article.)

From the poles it is immediate to calculate the natural frequencies and damping factors:

$$w_{nk} = |p_k|$$
$$\zeta_k = -\frac{Re[p_k]}{w_{nk}} \tag{7}$$

The numerical values are as follows:

$$w_{n1} = 6.273\,\text{rad/s};\ w_{n2} = 17.01\,\text{rad/s};\ w_{n3} = 23.90\,\text{rad/s}$$
$$\zeta_1 = 0.03137;\ \zeta_2 = 0.08506;\ \zeta_3 = 0.1195 \tag{8}$$

Secondly, the real part and the imaginary part of the FRFs measured are adjusted by least squares to a rational expression function of the calculated poles (see Fig. 3), which allows the measured residues to be estimated:

$$r_{11}^{(1)} = -0.01429 - 9.116i$$
$$r_{11}^{(2)} = -0.049 - 11.56i \tag{9}$$
$$r_{11}^{(3)} = -0.0618 - 10.41i$$

They are not the residues of the complex function in the s-domain, it is necessary to divide by f_s or multiply by T_s:

$$\hat{R}_{11}^{(1)} = -7.145 \cdot 10^{-6} - 0.004558i$$
$$\hat{R}_{11}^{(2)} = -2.45 \cdot 10^{-5} - 0.005781i \tag{10}$$
$$\hat{R}_{11}^{(3)} = -3.09 \cdot 10^{-5} - 0.005207i$$

note that the real part is practically of negligible value. All residues matrix terms for this case are included in Annex A. Once the poles and residues are known, the system is identified by Eq. (4).

It can be seen in Fig. 4 that the fit is very good.

3.2.1. System simulations/predictions (proportional damping)

Next, once the system is adjusted, the response to any type of load is simulated. First, the response of the system is calculated for a sinusoidal force applied in degree of freedom 3 with excitation frequencies of 1.5 Hz and 4.0 Hz (see Fig. 5):

$$u_3(t) = \sin(2\pi 1.5t) + \sin(2\pi 4.0t) \tag{11}$$

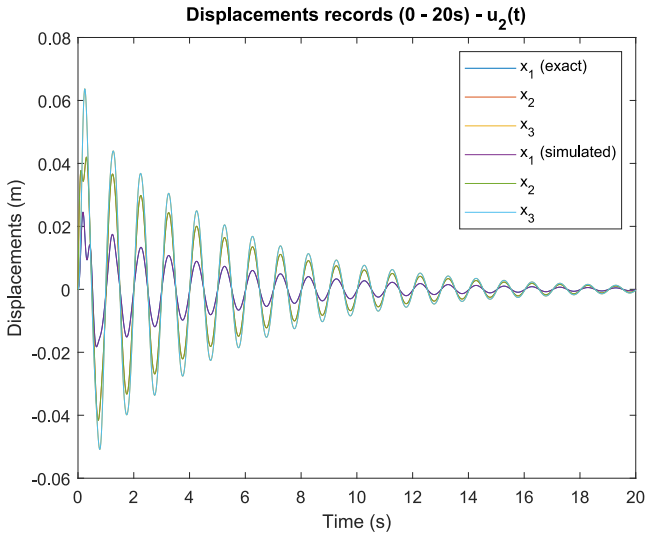

Fig. 4. Displacements records, impulse force at 2. (For interpretation of the references to color in this figure legend, the reader is referred to the web version of this article.)

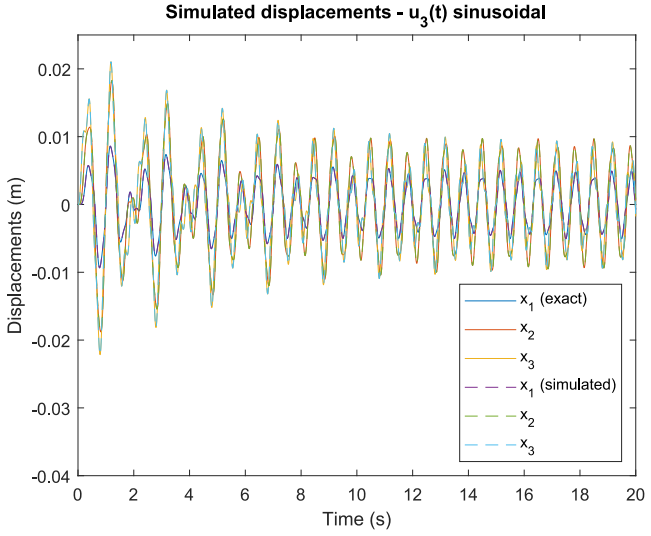

Fig. 5. Simulated displacements, sinusoidal force at 3. (For interpretation of the references to color in this figure legend, the reader is referred to the web version of this article.)

And secondly, the excitation is modified to sweep the frequencies from the frequency $f_1 = 0.2$ Hz to the value $f_2 = 10.0$ Hz applied in degree of freedom 2 during $t_1 = 20$ s (see Fig. 6):

$$u_2(t) = 10.0\sin((2\pi f_1 + 2\pi(f_2 - f_1)/t_1 \cdot t) \cdot t) \tag{12}$$

Once again it is verified that the correlation between the exact dynamic solution and the simulated one is very high.

3.3. General damping case

In this section the methodology is applied again but for the case of general damping. Fig. 7 shows the synthetic displacements records that correspond to the case of general damping, impulse input at node 1 (sampling rate f_s). The estimated poles of the system are:

$$p_1 = -0.6884 + 6.258i$$
$$p_2 = -1.254 + 17.38i \tag{13}$$
$$p_3 = -2.724 + 23.09i$$

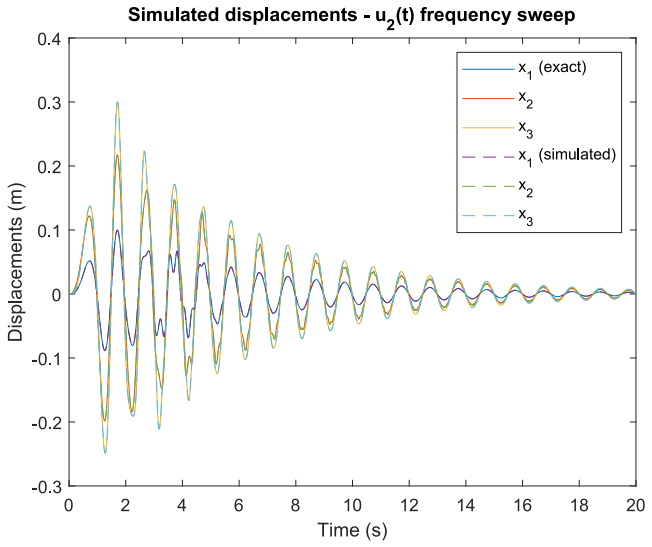

Fig. 6. Simulated displacements, frequency sweep at 2. (For interpretation of the references to color in this figure legend, the reader is referred to the web version of this article.)

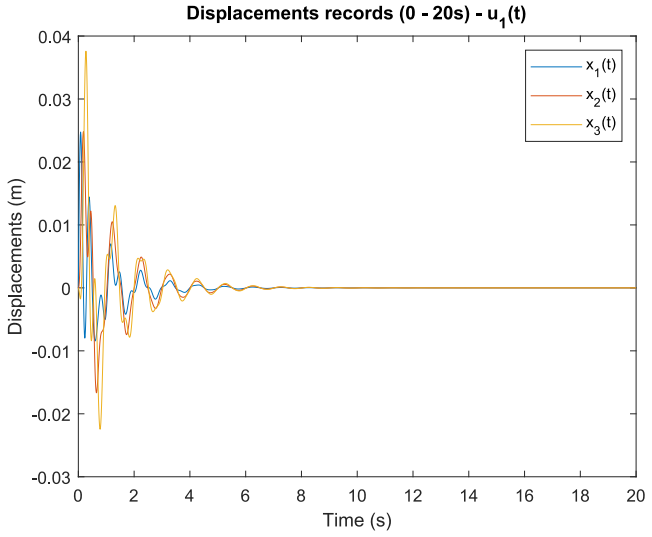

Fig. 7. Displacements records, impulse force at 1. (For interpretation of the references to color in this figure legend, the reader is referred to the web version of this article.)

Secondly, the real part and the imaginary part of the FRFs measured are adjusted (see Fig. 8), and the measured residues may be estimated:

$$\begin{aligned} r_{11}^{(1)} &= 0.01169 - 9.212i \\ r_{11}^{(2)} &= 5.719 - 12.37i \\ r_{11}^{(3)} &= -5.856 - 9.468i \end{aligned} \tag{14}$$

The measured residues are multiplied by T_s to obtain the residues of interest:

$$\begin{aligned} \hat{R}_{11}^{(1)} &= 5.845 \cdot 10^{-6} - 0.004606i \\ \hat{R}_{11}^{(2)} &= 0.002859 - 0.006187i \\ \hat{R}_{11}^{(3)} &= -0.002928 - 0.004734i \end{aligned} \tag{15}$$

All residues matrix terms are included in Annex A and Eq. (4) defines the dynamic system in terms of transfer function.. Again, graphically it can be seen that the fit is very good.

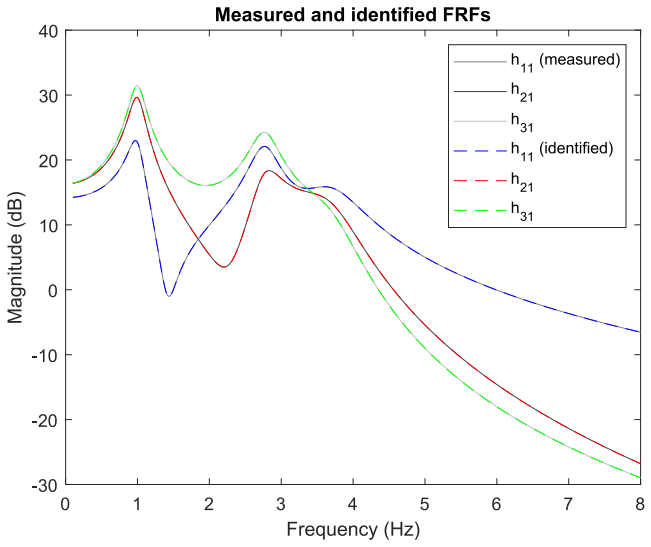

Fig. 8. Measured and identified FRFs (general damping). (For interpretation of the references to color in this figure legend, the reader is referred to the web version of this article.)

3.3.1. *System simulations/predictions (general damping)*

The response of the system with general damping is simulated for a sinusoidal force applied in degree of freedom 3 with excitation frequencies of 1.5 Hz and 4.0 Hz (see Fig. 9).

And secondly, the excitation is modified to sweep the frequencies from the frequency $f_1 = 0.2$ Hz to the value $f_2 = 10.0$ Hz applied in degree of freedom 2 during $t_1 = 20$ s (see Fig. 10):

In practice it is not necessary to know the mass, damping and stiffness matrices. This is for simplicity and as a check, but the methodology is general. The necessary information is the accelerations and forces at the points of interest, to which the methodology of this work is applied to predict the behavior of the dynamic system.

On the other hand, the driving point must always be considered to scale the problem and reproduce the dynamic of that specific system and not of all its equivalents. That is, systems whose dynamic behavior is similar although they have different masses (for example).

4. Conclusions

In this work, accelerations due to an impact (synthetic data) are measured in one of the degrees of freedom (in total three) and converted to displacements. It is analyzed in the frequency domain (s-domain, complex frequency) to obtain the poles and residues of the system and obtain a representation in the form of a transfer function matrix of the dynamic system identified.

A great contribution is that a direct relationship has been found between the measured residues and the residues of the complex functions defined in the s domain, complex frequencies. This allows the dynamic system to be identified quickly and intuitively by its frequency response from the applied forces and the acceleration records measured by the sensors.

System identifying as Frequency Functions Matrix response makes it easier to move on to other representations of the dynamic system: poles and residues; state space model and zeros, poles and gains. Simulate/predict the system dynamic response for other input/forces signals it is now possible.

Finally, this work can help describe systems using perfectly defined mathematical functions and not as black boxes that relate inputs and outputs. This can facilitate advances in the development and applications of Artificial Intelligence (AI) and Neural Networks (NNs).

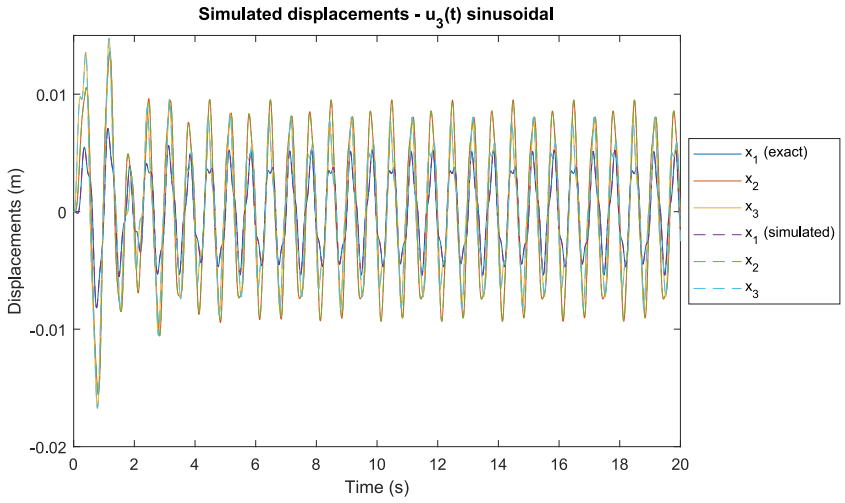

Fig. 9. Simulated displacements, sinusoidal force at 3. (For interpretation of the references to color in this figure legend, the reader is referred to the web version of this article.)

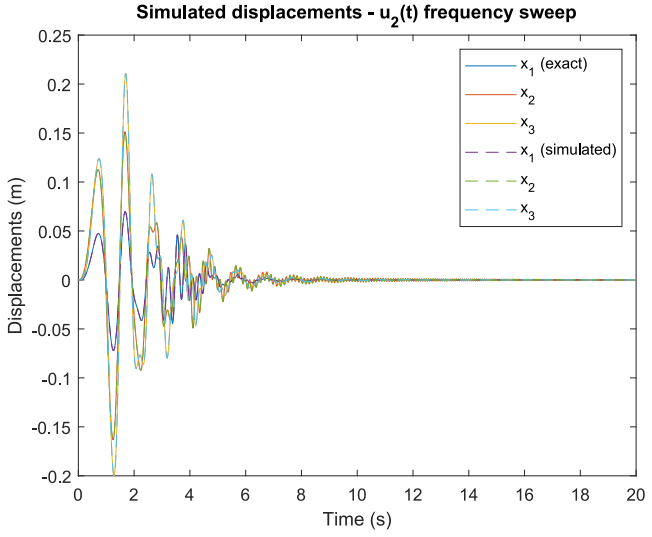

Fig. 10. Simulated displacements, frequency sweep at 2. (For interpretation of the references to color in this figure legend, the reader is referred to the web version of this article.)

Declaration of competing interest

The authors declare that they have no known competing financial interests or personal relationships that could have appeared to influence the work reported in this paper.

Acknowledgments

The author wishes to acknowledge to AEI, the Spanish government (10.13039/501100011033), and "ERDF A way of making Europe", for the partial support through the PID2022-140117NB-I00 Research Project.

Annex A. Auxiliary results

Proportional damping case (estimated values):

$$ {}_1\hat{\boldsymbol{A}}_{ij} = \begin{bmatrix} -7.145\cdot10^{-6} - 0.004558i & -1.61\cdot10^{-5} - 0.01027i & -2.005\cdot10^{-5} - 0.01279i \\ -1.61\cdot10^{-5} - 0.01027i & -3.63\cdot10^{-5} - 0.02316i & -4.519\cdot10^{-5} - 0.02883i \\ -2.005\cdot10^{-5} - 0.01279i & -4.519\cdot10^{-5} - 0.02883i & -5.627\cdot10^{-5} - 0.03589i \end{bmatrix} \tag{16} $$

$$ {}_2\hat{\boldsymbol{A}}_{ij} = \begin{bmatrix} -2.45\cdot10^{-5} - 0.005781i & -1.693\cdot10^{-5} - 0.003995i & 3.786\cdot10^{-5} + 0.008933i \\ -1.693\cdot10^{-5} - 0.003995i & -1.17\cdot10^{-5} - 0.00276i & 2.616\cdot10^{-5} + 0.006173i \\ 3.786\cdot10^{-5} + 0.008933i & 2.616\cdot10^{-5} + 0.006173i & -5.85\cdot10^{-5} - 0.0138i \end{bmatrix} \tag{17} $$

$$ {}_3\hat{\boldsymbol{A}}_{ij} = \begin{bmatrix} -3.09\cdot10^{-5} - 0.005207i & 3.306\cdot10^{-5} + 0.005571i & -1.781\cdot10^{-5} - 0.003002i \\ 3.306\cdot10^{-5} + 0.005571i & -3.538\cdot10^{-5} - 0.005962i & 1.906\cdot10^{-5} + 0.003212i \\ -1.781\cdot10^{-5} - 0.003002i & 1.906\cdot10^{-5} + 0.003212i & -1.027\cdot10^{-5} - 0.001731i \end{bmatrix} \tag{18} $$

General damping case (estimated values):

$$ {}_1\hat{\boldsymbol{A}}_{ij} = \begin{bmatrix} 5.845\cdot10^{-6} - 0.004606i & 0.0003014 - 0.01038i & -0.0003819 - 0.01292i \\ 0.0003014 - 0.01038i & 0.001328 - 0.02336i & -5.164\cdot10^{-5} - 0.02914i \\ -0.0003819 - 0.01292i & -5.164\cdot10^{-5} - 0.02914i & -0.002189 - 0.03623i \end{bmatrix} \tag{19} $$

$$ {}_2\hat{\boldsymbol{A}}_{ij} = \begin{bmatrix} 0.002859 - 0.006187i & -0.001396 - 0.004529i & -0.001592 + 0.01014i \\ -0.001396 - 0.004529i & -0.002826 - 0.001693i & 0.00389 + 0.005986i \\ -0.001592 + 0.01014i & 0.00389 + 0.005986i & -0.001875 - 0.01535i \end{bmatrix} \tag{20} $$

$$ {}_3\hat{\boldsymbol{A}}_{ij} = \begin{bmatrix} -0.002928 - 0.004734i & 0.001095 + 0.006163i & 0.001974 - 0.004276i \\ 0.001095 + 0.006163i & 0.001414 - 0.006895i & -0.0038380.00365i \\ 0.001974 - 0.004276i & -0.003838 + 0.00365i & 0.003939 + -0.0006035i \end{bmatrix} \tag{21} $$

References

[1] Meriam JL, Kraige LG. Engineering mechanics: Dynamics. John Wiley & Sons, Inc.; 2012.

[2] Andersson C, Ribeiro AH, Tiels K, Wahlström N, Schön TB. Deep convolutional networks in system identification. In: 2019 IEEE 58th conference on decision and control. 2019, p. 3670–6. http://dx.doi.org/10.1109/CDC40024.2019.9030219.

[3] Forgione M, Piga D. Continuous-time system identification with neural networks: model structures and fitting criteria. Eur J Control 2021;59:69–81. http://dx.doi.org/10.1016/j.ejcon.2021.01.008.

[4] Forgione M, Piga D. dynoNet: a neural network architecture for learning dynamical systems. Internat J Adapt Control Signal Process 2021;35(4):612–26. http://dx.doi.org/10.1002/acs.3216.
[5] Sjövall P, Abrahamsson T. Component system identification and state-space model synthesis. Mech Syst Signal Process 2007;21(7):2697–714. http://dx.doi.org/10.1016/j.ymssp.2007.03.002.
[6] Yu C, Ljung L, Verhaegen M. Identification of structured state-space models. Automatica 2018;90:54–61. http://dx.doi.org/10.1016/j.automatica.2017.12.023.
[7] Zhao W, Yin G, Bai EW. Sparse system identification for stochastic systems with general observation sequences. Automatica 2020;121:109162. http://dx.doi.org/10.1016/j.automatica.2020.109162.
[8] Mottershead JE, Friswell MI. Model updating in structural dynamics: a survey. J Sound Vib 1993;167(2):347–75. http://dx.doi.org/10.1006/jsvi.1993.1340.
[9] Lin RM. Function-weighted frequency response function sensitivity method for analytical model updating. J Sound Vib 2017;403:59–74. http://dx.doi.org/10.1016/j.jsv.2017.05.031.
[10] Ereiz S, Duvnjak I, Jiménez-Alonso JF. Review of finite element model updating methods for structural applications. Structures 2022;41:684–723. http://dx.doi.org/10.1016/j.istruc.2022.05.041.
[11] Modak SV, Kundra TK, Nakra BC. Comparative study of model updating methods using simulated experimental data. Comput Struct 2002;80(5):437–47. http://dx.doi.org/10.1016/S0045-7949(02)00017-2.
[12] Yang CD, Yeh FB. Identification, reduction, and refinement of model parameters by the eigensystem realization algorithm. J Guid Control Dyn 1990;13(6):1051–9. http://dx.doi.org/10.2514/3.20578.
[13] Chen SY, Ju MS, Tsuei YG. Estimation of mass, stiffness and damping matrices from frequency response functions. J Vib Acoust 1996;118(1):78–82. http://dx.doi.org/10.1115/1.2889638.
[14] De Angelis M, Lus H, Betti R, Longman RW. Extracting physical parameters of mechanical models from identified state-space representations. J Appl Mech 2002;69(5):617–25. http://dx.doi.org/10.1115/1.1483836.
[15] Ewins DJ. Modal testing: Theory, practice, and application. 2nd ed. Research Studies Press; 2000.
[16] Maia N, Silva J. Theoretical and experimental modal analysis. Engineering dynamics series, Research Studies Press; 1997.
[17] Yang K, Yu K, Li Q. Modal parameter extraction based on Hilbert transform and complex independent component analysis with reference. Mech Syst Signal Process 2013;40(1):257–68. http://dx.doi.org/10.1016/j.ymssp.2013.05.003.
[18] Tang D, Sun X, Yue Q, Shi Z, Feng J. Research of complex modal parameters extraction of a multi-degree-of-freedom structure based on similarity search. Ocean Eng 2015;108:307–14. http://dx.doi.org/10.1016/j.oceaneng.2015.07.060.
[19] Lu ZR, Lin G, Wang L. Output-only modal parameter identification of structures by vision modal analysis. J Sound Vib 2021;497:115949. http://dx.doi.org/10.1016/j.jsv.2021.115949.
[20] Wang G, Li H, Fu Z, Huang W, Liu B, Yaom S. A novel methodology for modal parameter identification of arch dam based on multi-level information fusion. Mech Syst Signal Process 2023;183:109578. http://dx.doi.org/10.1016/j.ymssp.2022.109578.
[21] Cukor I, Seles K, Tonkovic Z, Peric M. An inverse approach for load identification of cracked wind turbine components. Energy Sources A: Recovery Util. Environ. Effects 2023;45(1):962–84. http://dx.doi.org/10.1080/15567036.2021.1982077.
[22] Liu Y, Wang L, Feng B. Load-independent multi-objective sensor placement method for localization and reconstruction of external excitations under interval uncertainties. Comput Methods Appl Mech Engrg 2023;416:116344. http://dx.doi.org/10.1016/j.cma.2023.116344.
[23] Ganaie M, Hu M, Malik A, Tanveer M, Suganthan P. Ensemble deep learning: A review. Eng Appl Artif Intell 2022;115:105151. http://dx.doi.org/10.1016/j.engappai.2022.105151.
[24] Liu Y, Wang L, Feng B. A hybrid model-data-driven framework for inverse load identification of interval structures based on physics-informed neural network and improved Kalman filter algorithm. Appl Energy 2024;359:122740. http://dx.doi.org/10.1016/j.apenergy.2024.122740.
[25] Dong YR, Xu ZD, Li QQ, He ZH, Yan X, Cheng Y. Tests and micro–macro cross-scale model of high-performance acrylate viscoelastic dampers used in structural resistance. J Struct Eng 2023;149(7). http://dx.doi.org/10.1061/JSENDH.STENG-11767.
[26] Cleve BM. Numerical Computing with MATLAB. Society for Industrial and Applied Mathematics; 2004.
[27] Gilat A. MATLAB: An introduction with applications. John Willey & Sons, Inc.; 2005.
[28] Verboven P. Frequency domain system identification for modal analysis [Ph.D. thesis], Vrije Universiteit Brussel; 2002.
[29] Guillaume P, Verboven P, Cauberghe B, Vanlanduit S, Parloo E, Sitter G. Frequency-domain system identification techniques for experimental and operational modal analysis. IFAC Proc Vol 2003;36(16):1609–14. http://dx.doi.org/10.1016/S1474-6670(17)34990-X, 13th IFAC Symposium on System Identification (SYSID 2003), Rotterdam, The Netherlands, 27-29 August, 2003.
[30] Meirovitch L. Elements of vibration analysis. McGraw-Hill; 1986.